

## Multifunctional Anti-Reflective, Self-Cleaning and UV Protection Coatings Made of Electrodeposited Nanostructured ZnO Arrays in Pulsed Mode

<sup>1</sup>V.V. Ivanov, <sup>1</sup>G.V. Tsepilov, <sup>2</sup>N.V. Porfirov and <sup>1</sup>A.N. Voropai

<sup>1</sup>CJSC “TECHNOCOMPLEKT”, Shkolnaya Street 10a, Dubna, 141981 Moscow Oblast, Russia

<sup>2</sup>ООО “TURBOENERGOREMONT”, Premises 170N, Block A, 114 Leninskii Prospect,  
Saint Petersburg, 198207 Leningradskaya Oblast, Russia

**Abstract:** In this study, it is proposed to use the method of pulsed cathodic deposition to manufacture anti-reflective, self-cleaning and UV protective nanostructured zinc oxide layers, since this method has additional possibilities for varying the morphology, the structure and the properties of coatings as compared with the commonly used constant-current electrodeposition. The analysis was carried out for optical properties, crystal structure, substructural parameters and the texture of silicon plates electrodeposited in pulsed mode on the surface for nanostructured zinc oxide arrays. The anti-reflective properties of ZnO arrays were demonstrated on Si surface. The development of single-phase ZnO nanostructures with a characteristic texture in <001> direction was determined. The result of the wettability study is a high hydrophobicity of ZnO surfaces which is regulated by the exposure to ultraviolet irradiation. It was shown that such surfaces are self-cleaning ones with the “rose petal effect” and are able to protect Si surface from the destructive action of the solar spectrum ultraviolet part.

**Key words:** Pulsed electrodeposition, ZnO, self-cleaning, antireflection effect, “rose petal effect”

---

### INTRODUCTION

The development of highly hydrophobic self-cleaning antireflective and UV-resistant coatings is an urgent problem that must be solved in the process of modern solar energy product, electronics and optical electronics manufacturing. According to Gao *et al.* (2011, 2014), the design and the development of self-cleaning coatings is especially important for the use in Solar Batteries (SB), given that SBs lose almost half of the total solar energy conversion efficiency annually because of dust accumulation. Other sources of SB efficiency loss are the degradation of base semiconductor layers due to the action of solar spectrum ultraviolet radiation and an incomplete assimilation of solar energy as the result of an optical reflection effect (Gao *et al.*, 2014; Hiralal *et al.*, 2014; Hussain *et al.*, 2015; Aurang *et al.*, 2013; Liu *et al.*, 2011).

Among the possible ways of this problem elimination, the most promising approach is the development of array products from Zinc Oxide (ZnO) nanorods using inexpensive liquid-phase chemical and electrochemical methods suitable for large-scale production (Gao *et al.*, 2014; Hiralal *et al.*, 2014; Hussain *et al.*, 2015; Aurang *et al.*, 2013; Liu *et al.*, 2011).

This approach turned out to be especially effective for silicon SB (Hussain *et al.*, 2015; Aurang *et al.*, 2013; Liu *et al.*, 2011) but there is no unified opinion concerning the ways of its implementation now a days.

It is known that superhydrophobicity and self-cleaning are provided both by the chemical composition of surfaces and by their morphology. If the contact angle that a liquid drop is developed with a solid substrate (wetting angle)  $\theta > 90^\circ$  then such a surface is called hydrophobic one. The water on it is collected in drops. High hydrophobic and superhydrophobic nanostructured materials have  $\theta > 120^\circ$  and  $\theta > 150^\circ$ , respectively. They are characterized by the effects of self-cleaning, water repellency, anti-icing and anti-fogging which are necessary in a number of electronic devices and optical devices, including solar cells (Bhushan *et al.*, 2009). Since such surfaces are widespread in nature, the effects caused by them are associated with natural objects specifically. For example, “lotus leaf” effect corresponds to the situation when droplets roll down or slide easily over a superhydrophobic solid surface (Bhushan and Jung, 2011; Lam *et al.*, 2002). If well-formed drops are retained firmly on a vertical wall or can be suspended even to a solid surface from below, then they say about super hydrophobicity with the “rose petal

effect" (Yan *et al.*, 2011; Myint *et al.*, 2014; Guo *et al.*, 2011). With the "rose petal effect" the drops are pinned to a surface (Myint *et al.*, 2014; Guo *et al.*, 2011; Lam *et al.*, 2002; Quere, 1998).

Two approximations are used to describe theoretically the contact of a liquid droplet with a nanostructured solid surface: the Wenzel state and the Cassie mode, i.e., the Cassie-Baxter regime. If water penetrates into the cavities of nanostructures and fills them Wenzel's state takes place (Lam *et al.*, 2002). It is characterized by hydrophilicity or usual hydrophobicity. At the maximum slope of the surface above which the drop begins to slide or roll in the Wenzel Mode the approaching (lower) contact angle of the drop is much larger than its retreating (upper) contact angle, the difference between these angles called wetting hysteresis  $\Delta\theta$  is large, self-cleaning is not carried out.

If superhydrophobicity of the surface is manifested not only in a large wetting angle (often  $\theta > 150^\circ$ ) but also in a small wetting hysteresis  $\Delta\theta < 10^\circ$  then the Cassie Mode (Cassie-Baxter) takes place. According to Zhang *et al.* (2004), the Cassi regime is characterized by wetting hysteresis  $\Delta\theta = 8^\circ$  and according to Bhushan and Jung (2011),  $\Delta\theta < 1^\circ$ . In Cassie situation, the water drops are located both on the upper sections of the solid nanostructures and on the air bubbles in their voids which drops are unable to take out of these voids. Due to the weak adhesion of a droplet with a solid matter, it rapidly slips or slides off the surface even at a slight inclination ( $\sim 4^\circ$ ), capturing the impurities which ensures the self-cleaning of the surface with the "lotus effect" (Quere, 1998) or in other words, Cassie sliding mode. In order to achieve the state of superhydrophobicity with the "lotus effect" the nanostructured surfaces, like natural objects are modified, additionally applying water repellent coatings on them in the form of ultrathin layers from the compounds with low surface free energy, most often from fluorinated silanes or alkylsilanes (Zhang *et al.*, 2004). The literature describes nanostructured layers of zinc oxides that are capable to exhibit high hydrophobicity and superhydrophobicity being additionally treated with third-party substances for the purpose of application in micro and nanoelectronics (Zhang *et al.*, 2004). Nevertheless, Cassie's superhydrophobicity regime is usually unstable and prone to full or partial conversion to Wenzel's regime, for example, under the influence of pressure, heating, vibration or when a droplet evaporates (Bhushan and Jung, 2011).

The "rose petal effect" is observed in the case (Yan *et al.*, 2011) when only large irregularities are completely filled with water in spite of solid surface high hydrophobicity and some small irregularities are filled only partially and there is little air in them. "The rose petal

effect" corresponds to the mixed Wenzel-Cassie regime well described by Gao *et al.* (2011), the self-cleaning of surfaces with this effect occurs when the surface becomes hydrophilic under the action of the UV spectrum and therefore a droplet spreads out. According to Liu *et al.* (2004), the reason of surface self-cleaning with the "rose petal effect" under the influence of solar spectrum UV radiation is the oxidation and partial decomposition of organic contaminants, after which they were easily washed off by rain from hydrophilic zinc oxide nanostructures. Liu *et al.* (2004) and Barreca *et al.* (2009) found that the super-hydrophilicity induced by ultraviolet turns into the original superhydrophobicity, if the zinc oxide nanostructures are in the dark. By Yan *et al.* (2011), this ability of highly hydrophobic ZnO nanostructures with the "rose petal effect" converted reversibly under the influence of ultraviolet irradiation into superhydrophilic ones was used for the self-cleaning of nanoelectronic device surfaces.

The interest in nanostructured ZnO layers is also caused by the possibility of their use as the protection from ultraviolet radiation in addition to high hydrophobicity and self-cleaning. As was shown by the researchers (Liu *et al.*, 2004), the surface of ZnO nanorod arrays is capable of reversible transformation from highly hydrophobic to hydrophilic under the influence of UV and the reason for this metamorphosis is the ability of UV irradiation to generate electron-hole pairs in zinc oxide. The result of holes and nodular oxygen interaction is the appearance of surface oxygen vacancies in ZnO which are filled with oxygen which arose as the result of water molecule dissociative adsorption from moist air and the surface of the nanostructures is covered with a large number of OH hydroxyl groups, i.e., becomes hydrophilic. Thus the UV energy is not spent on the degradation of the underlying base layers but on the interaction with ZnO array.

In this study, we propose to use the method of pulsed cathodic deposition for the production of antireflection and UV-shielding nanostructured zinc oxide layers with high hydrophobicity controlled by ultraviolet irradiation, since this method has additional possibilities for varying the morphology, the crystal structure and the optical properties of nanostructures as compared with the commonly used constant-current electrodeposition.

## MATERIALS AND METHODS

**Experiment procedure:** The production of zinc oxide nanorod arrays was performed by pulsed cathodic electrochemical deposition in a thermostated three electrode electrochemical cell with an immiscible aqueous electrolyte containing 0.01 M of  $\text{Zn}(\text{NO}_3)_2$  and 0.1 M of  $\text{NaNO}_3$  at the temperature of  $70^\circ\text{C}$ . The polished silicon plates KDB-10 with embedded p-n<sup>+</sup> heterojunctions at the

depth of 1.6-1.8  $\mu\text{m}$  were used as substrates (cathodes or working electrodes). A platinum helix served as a counterelectrode and chlorine-silver Ag/AgCl electrode served as a reference electrode. In the process of nanostructured zinc oxide array fabrication a nanosized germinal ZnO sublayer was created during the first stage of electrodeposition by the feeding of the same electrolyte on a working electrode in the form of a Si plate with a p-n<sup>+</sup> for 30 sec by the heterojunction of the constant potential  $U = -1.3$  V. After this, using the Potentiostat PI-50-1.1, equipped with the programmer PR-8, rectangular potential pulses were fed to the cathode substrate for pulsed electrolysis performance during 1-30 min: the lower limit of the cathode potential  $U_{\text{off}}$  was -0.7 V, the upper limit  $U_{\text{on}} = -1.3$  V (Potentials are given relative to the Ag/AgCl reference electrode). The duty cycle, that is the ratio of the pulse duration to the sum of the pulse and pause duration and the frequency as the value reciprocal of the sum of pulse and pause duration were 0.4 and 2 Hz, respectively.

The study of nanostructured zinc oxide layer optical properties was performed using SF-2000 spectrophotometer equipped with a mirror and diffuse reflection attachment SFO-2000. The light scattering factor (Hf) was calculated as the ratio of the diffuse reflection  $R_d$  to the total reflection  $R$  (the sum of diffuse  $R_d$  and mirror  $R_s$  reflections). The measurements of  $R_d$  and  $R_s$  were carried out at the angles of light incidence relative to the normal of substrate surface  $\theta$  in the range of 8-45°. The thicknesses of  $d_{\text{ZnO}}$  of ZnO layers were determined using the interference peaks on the mirror reflection spectra  $R_s(\lambda)$  similar to (Chowdhury, 2011):

$$d_{\text{ZnO}} = \frac{\Delta m}{2\sqrt{n_1^2 - \sin^2 \theta}} \frac{\lambda_1 \lambda_2}{\lambda_2 - \lambda_1} \quad (1)$$

Where:

- $\theta$  = The angle of light incidence relative to the normal of the sample substrate
- $\lambda_1$  and  $\lambda_2$  = The wavelengths corresponding to the maxima in the mirror reflection spectrum
- $n_1$  = The average refractive index of ZnO in the wavelength interval  $\lambda_1$  and  $\lambda_2$
- $\Delta m$  = The number of maxima between  $\lambda_1$  and  $\lambda_2$

In order to analyze the structural and substructural parameters of ZnO arrays, X-Ray spectra (XRD) were recorded using a DRON-4 diffractometer in  $\text{CoK}\alpha$  radiation ( $\lambda_{\text{CoK}\alpha} = 1.7889 \text{ \AA}$ ). The scanning was performed during bragg-brentano focusing. The processing of the obtained X-ray diffractograms (separation of the background, separation of the doublet  $\text{K}\alpha_1$ - $\text{K}\alpha_2$ , etc.) as well as the calculation of diffraction line profile parameters were carried out using the programs

“New-profile v.3.4 (486)” and “OriginPro v.7.5”. The presence of crystalline phases was detected by the comparison of experimental X-ray diffraction patterns with the reference data base JCPDS using the program “PCPDFWIN v.1.30”. The estimation of Coherent Scattering Regions (CSR) and microstresses  $\Delta d/d$  (where  $d$  is the crystal lattice period according to JCPDS,  $\Delta d$  is the difference between the experimental and the reference value of the lattice period) in the zinc oxide arrays was performed by the analysis of X-ray diffraction maxima broadening by Williamson-Hall approximation method according to Quere (1998). The residual stresses  $\sigma$  in zinc oxide arrays were calculated on the basis of data about electrodeposited  $c$  and reference  $c_{\text{bulk}}$  samples of a lattice period using the values of material elasticity constants in different directions:

$$\sigma = -233 \times \frac{c - c_{\text{bulk}}}{c_{\text{bulk}}}; c_{\text{bulk}} = 5.206 \quad (2)$$

The crystal lattice parameters  $a$  and  $c$  of zinc oxide hexagonal phase were calculated according to Quere (1991). According to the position of the last two indexed X-ray diffraction lines using Nelson-Rilli graphical extrapolation they were cleared by the Least Squares Method (LSM) using the unit cell program with the use of all registered reflections of X-ray diffraction patterns.

In order to study the texture of electrodeposited zinc oxide arrays according to Harris method they used the values of X-ray diffractometric peak integrated intensities in accordance with. For each peak they calculated the value of the pole density  $p(hkl)$  was calculated which characterizes the probability with which the normal to the crystallite surface coincides with the normal to  $(hkl)$  plane, that is, it determines the number of crystallites the  $(hkl)$  planes of which are parallel to a sample surface. The pole densities were calculated for all recorded x-ray diffractometric peaks, the values of  $p(hkl) > 1$  were attributed to the texture axes.

In order to analyze the hydrophobicity/hydrophilicity of nanostructured zinc oxide layer surface, standard sessile drop, tilt angle measurement and the observation of droplet evaporation were used well described by Bhushan *et al.* (2009) and Bhushan and Jung (2011). In the “sessile drop” method, the drop of distilled water with the radius  $r$  from 0.7-1 mm and the volume of 1.5-3.7  $\mu\text{L}$  was placed on a horizontal surface of Si with ZnO layer using a syringe. Water droplets were applied at five different points of ZnO sample surface during each analysis in order to increase the drop measurement accuracy. The fixation of a drop image during its drying on the surface was carried out using Samsung PL55 digital camera, the lens of which was placed at the level of the

surface using a tripod. In order to determine the hysteresis of the wetting  $\Delta\theta$ , Si surface with ZnO layer and a drop of water were inclined. The angles of inclination with respect to TA horizon were 7-32°. After that, the drop was photographed and its retreating (upper) and upcoming (lower) contact angles were measured. In order to observe the evaporation of water droplets on the surface of nanostructured ZnO layers, the series of drops were created for 4 min, the survey was performed every 60 sec. The determination of the contact angle on the horizontal surface  $\theta$  as well as of the approaching and receding marginal angles on the inclined ZnO/Si surface was carried out by analyzing the drop profile on the images in accordance with the procedure (Bhushan *et al.*, 2009; Bhushan and Jung, 2011; Bhushan, 2011) in order to establish the wetting characteristics. The edge angle was calculated in accordance with (Bhushan and Jung, 2011; Bhushan, 2011) using the following Eq. 3:

$$\text{tg}(\theta/2)h/r \quad (3)$$

Where:

h = The height of the drop above the surface

r = The radius of the drop base lying on ZnO surface

The volume of the drop was determined by conventional geometric formulas depending on its shape to calculate the volume of a sphere or its segment. The study of ZnO surface wetting properties change under the influence of ultraviolet irradiation from a highly hydrophobic state to a hydrophilic one was carried out by a surface illumination with ZnO layer by UV lamp of 26 W. The wavelength of UV radiation made 315-400 nm. UV irradiation of ZnO was carried out for 10-60 min. After the keeping of the samples under the influence of UV-irradiation in the indicated time interval, the record of a droplet profile was performed using a digital camera. In order to observe the restoration of ZnO surface highly hydrophobic state after its UV irradiation the samples were kept in the dark for 14 days, the drop profiles were photographed every 2 days.

## RESULTS AND DISCUSSION

Figure 1 shows the results of optical studies concerning the nanostructured zinc oxide arrays electrodeposited in pulsed mode on polished silicon plates. According to Fig. 1, electrodeposited ZnO arrays make a significant antireflection effect at any angles of light incidence  $\theta$ , reducing both the mirror reflection  $R_s$  and the total reflection  $R$ . According to Hiralal *et al.* (2014) this effect is characteristic of anti-reflective coatings from

the arrays of zinc oxide nanostructures, since it provides an effective refractive index between air and Si. Depending on the electrodeposition period ZnO nanostructures have averaged thicknesses of 80 nm (at the deposition time of 1 min), 400 nm (at the deposition time of 5 min) and 1200 nm (at the deposition time of 30 min). The reflection spectra of thicker ZnO arrays on Fig. 1a and b have interference extrema characteristic of ZnO nanorod layers deposited on the surface with a higher optical density which correspond to fabry-perot reflection oscillations, similar to those described by Hiralal *et al.* (2014). According to the spectra of light scattering factor  $H_f$  shown on Fig. 1c, the reflection from zinc oxide arrays has mainly diffuse character as is typical of one-dimensional nanostructures.

Figure 2 shows typical X-ray diffraction patterns of electrodes deposited on the surface of single-crystal silicon plates of nanostructured ZnO arrays with the thickness of 550-1200 nm. A halo is observed on the diffractograms which according to Klochko *et al.* (2013), is explained by the amorphization of silicon during the development of p-n<sup>+</sup> transitions by the thermal diffusion of phosphorus. The result of this thermal diffusion is the halo transformation into the series of disordered regions within the near-surface region of a single crystal Si. There are also peaks explained by the presence of various silicon phosphides created during the development of the n<sup>+</sup>-Si layer in the p-Si plate. According to X-ray diffractometry data, all the layers deposited on the silicon plates in terms of the phase composition were ZnO wurtzite modifications (JCPDS PDF#361451).

The results of structural and substructural characteristic analysis as well as the analysis of ZnO array axial texture with the thicknesses from 550-1200 nm are given in Table 1. The electrodeposited zinc oxide arrays are nanocrystalline ones and they are all characterized by insignificant microstresses  $\Delta d/d \approx 10^{-3}$ . The residual compressive stresses range from -0.22 to 0.59 GPa and are increased with the increase of ZnO array thickness. The calculations showed that the electrodeposited ZnO nanostructures are characterized by increased crystal lattice parameters along the axis c as compared to the reference ZnO (in accordance with JCPDS PDF # 361 451, c = 5.207 Å). All ZnO arrays are textured in the <001> direction, that is they are perpendicular to a substrate surface and the texture perfection indicator-polar density p (002) increases with the array thickness increase that is during the growing of zinc oxide nanorods.

The results of surface wettability study concerning nanostructured ZnO arrays, electrodeposited in a pulsed mode on silicon wafers, demonstrated their high hydrophobicity. The example shown on Fig. 3a of such a

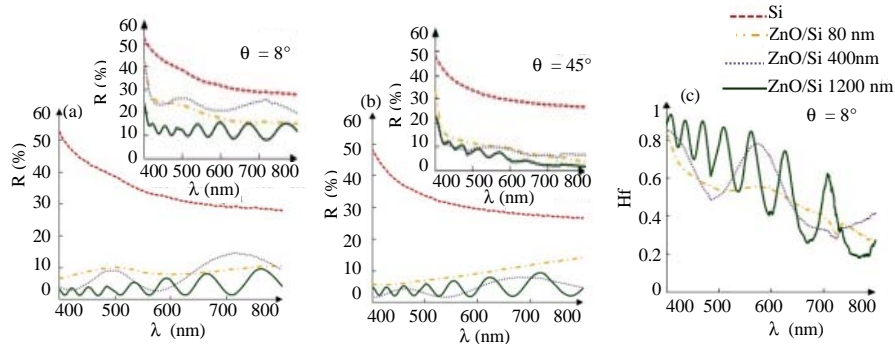


Fig. 1: The spectra of mirror reflection  $R_s$  (a, b) and total reflection  $R$  (on inserts) of electrodeposited nanostructured ZnO arrays in pulsed mode on silicon substrates at light incident angles relative to the substrate surface normal  $\theta = 8^\circ$  (a) and  $\theta = 45^\circ$  (b). The spectrum of the light scattering factor  $H_f$  at  $\theta = 8^\circ$  (c)

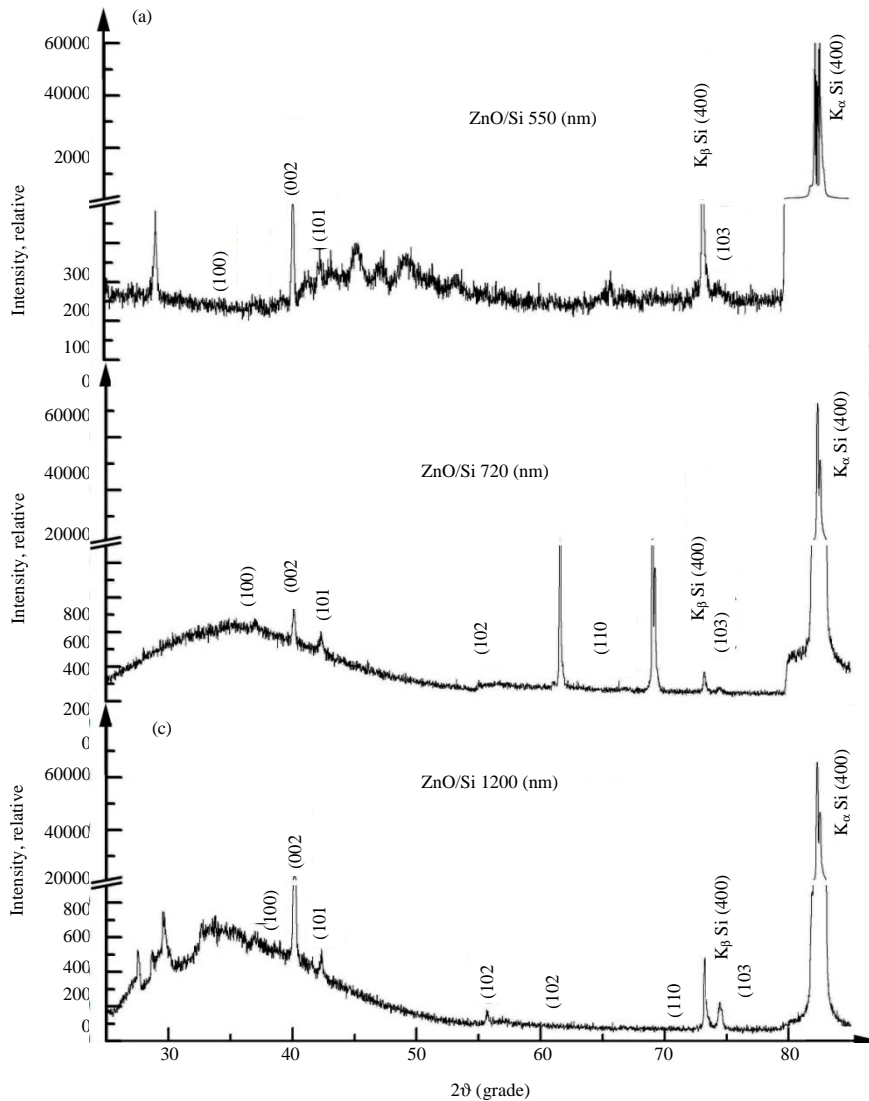


Fig. 2: a-c) X-ray diffraction patterns of nanostructured zinc oxide arrays electrodeposited in pulsed mode on Si substrates (The averaged thicknesses of ZnO are indicated)

Table 1: Structural, substructural parameters and the texture of electrodeposited ZnO arrays on Si plates in pulsed mode (according to X-ray diffractometry data)

				Grid parameters (Å)					
				Nelson-Rilly Method		MNK		Texture	
ZnO array thickness	OKR (nm)	$\Delta d/d \times 10^3$	$\sigma$ (Gpa)	a	c	a	c	Polar density ( $P_{\text{hkl}}$ )	h k l
550	40-60	0.6-1,9	-0.22	3.256	5.208	3.247	5.211	1.87	
720	80-200	0.5-1,4	-0.27	3.244	5.223	3.249	5.212	2.35	(002)
1200	70-200	1.3-2.3	-0.59	3.246	5.236	3.244	5.219	4.13	

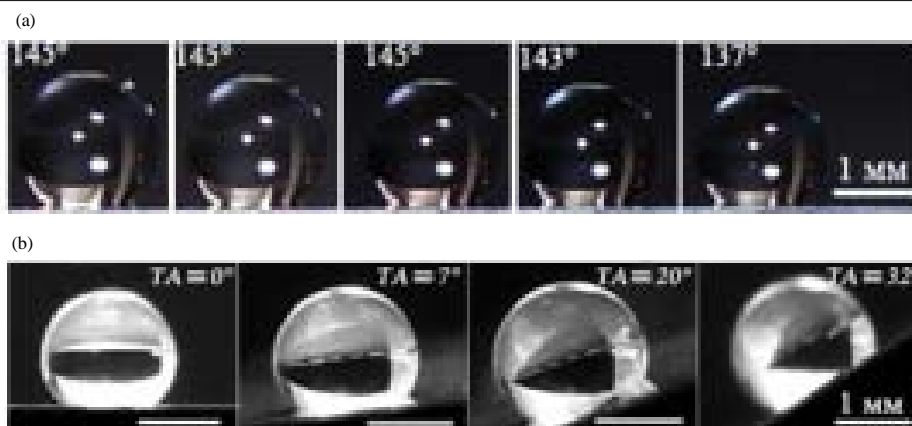


Fig. 3 a): The series of water drop photos on a ZnO/Si surface for an electrodeposited, ZnO array with the thickness of 720 nm in a pulsed mode, fixed as the droplet dries out every 60 sec. The values of the edge angle  $\theta$  determined by the Eq. 3 are indicated in the corners of the photographs; b) A series of water drop photographs on the same ZnO/Si surface at different tilting angles of a plate  $TA = 0^\circ, 10^\circ, 20^\circ, 30^\circ$

surface (ZnO/Si) is characterized by the contact angle  $\theta = 145^\circ$ . According to Quere (1998), Shirtcliffe *et al.* (2010), the observations of droplet evaporation “sitting” on a horizontal surface, allow to determine the character of wetting according to the shape of contact angle  $\theta$  dependences on the volume of drops  $V$ . According to Shirtcliffe *et al.* (2010), if the function  $\theta(V)$  has the form of a horizontal straight line, then the Cassie mode takes place at which water does not penetrate into the voids between the irregularities which is manifested in the superhydrophobicity with the “lotus effect” that is a drop going down is observed at a slight surface inclination. If the dependence  $\theta(V)$  decreases monotonically with  $V$  decrease then we have Wenzel regime or a mixed Wenzel-Cassie regime according to Shirtcliffe *et al.* (2010) with characteristic hysteresis wettability  $\Delta\theta > 10^\circ$ . For the same surface a change of regime from Cassie to Wenzel can occur as  $V$  decreases. As can be seen on Fig. 3a, the highly hydrophobic ZnO/Si surface records a mixed Wenzel-Cassie wetting regime when a droplet dries up which is closer to Cassie, since  $\theta$  decreases but insignificantly. The studies of wetting hysteresis  $\Delta\theta$  by the method of inclination angle measuring showed (Fig. 3b) that the highly hydrophobic nanostructured ZnO

layers electrodeposited in pulsed regimes have the difference reaches  $24^\circ$  between the advancing and receding angles with the surface inclination of  $TA = 20-30^\circ$  to the horizon, the drops are firmly “pinned” to the surface. Thus the “rose petal effect” is observed among highly hydrophobic nanostructured ZnO layers electrodeposited by us in pulsed modes.

As shown on Fig. 4a, during ultraviolet irradiation of highly hydrophobic ZnO surfaces with the “rose petal effect” within 10-60 min their contact angle decreases monotonically until the hydrophilicity is reached. Let’s note that and (Liu *et al.*, 2004 and Barreca *et al.* (2009) UV irradiation lasted much longer to achieve the superhydrophilicity of ZnO, namely for 2-3 h. As can be seen on Fig. 4b, the change of electrodeposited surface wettability in the pulsed modes of nanostructured ZnO layers was a reversible one under the influence of ultraviolet irradiation. Thus, ZnO nanostructures produced by us represented an adaptive material capable of changing its properties under the influence of ultraviolet, thereby protecting the silicon layer from the destructive UV effect and at the same time capable of cleaning itself from dust according to the mechanism peculiar to superhydrophobic surfaces with the “rose petal effect”.

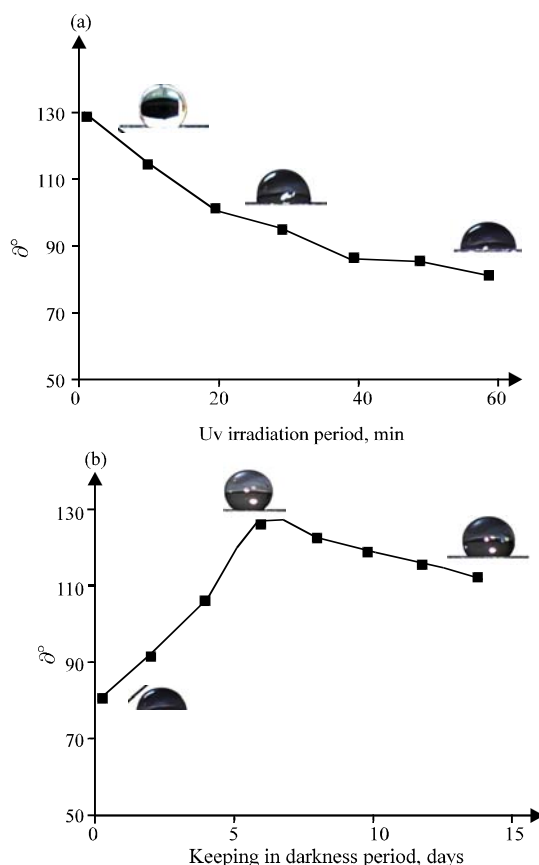


Fig. 4: a, b) Change of highly hydrophobic ZnO/Si surface wettability with the “rose petal effect” under the influence of their ultraviolet irradiation. The hydrophobicity restoration among these nanostructured ZnO arrays during their stay in the dark

## CONCLUSION

The analysis of optical properties, crystal structure, substructural parameters and the texture of nanostructured zinc oxide arrays electrodeposited in pulsed mode on the surface of silicon plates. Antireflective properties of ZnO arrays on the Si surface are demonstrated. The development of single-phase ZnO nanostructures with a characteristic texture in the  $\langle 001 \rangle$  direction was revealed. The result of wettability study showed high hydrophobicity of ZnO surfaces which is regulated by the exposure to ultraviolet irradiation. It was shown that such surfaces are self-cleaning ones with the “rose petal effect” and are able to protect the Si surface from the degrading effect of the solar spectrum ultraviolet part.

## ACKNOWLEDGEMENTS

This study was prepared as a part of the implementation of Applied Research and Experimental Development (ARED) on the agreement on the subvention (2015, October, 27) No. 14.579.21.0113 with the financial support of the Ministry of education and science of the Russian Federation. A unique identifier of ARED- RFMEFI57915X0113.

## REFERENCES

- Aurang, P., O. Demircioglu, F. Es, R. Turan and H.E. Unalan, 2013. ZnO nanorods as antireflective coatings for industrial scale single crystalline silicon solar cells. *J. Am. Ceram. Soc.*, 96: 1253-1257.
- Barreca, D., A. Gasparotto, C. Maccato, E. Tondello and U.L. Stangar *et al.*, 2009. Photoinduced superhydrophilicity and photocatalytic properties of ZnO nanoplatelets. *Surf. Coat. Technol.*, 203: 2041-2045.
- Bhushan, B. and Y.C. Jung, 2011. Natural and biomimetic artificial surfaces for superhydrophobicity, self-cleaning, low adhesion and drag reduction. *Prog. Mater. Sci.*, 56: 1-108.
- Bhushan, B., 2011. Biomimetics inspired surfaces for drag reduction and oleophobicity-philicity. *Beilstein J. Nanotechnol.*, 2: 66-84.
- Bhushan, B., Y.C. Jung and K. Koch, 2009. Micro-, nano- and hierarchical structures for superhydrophobicity, self-cleaning and low adhesion. *Philos. Trans. R. Soc. London A. Math. Phys. Eng. Sci.*, 367: 1631-1672.
- Chowdhury, F., 2011. Influence of thickness variation on the optical properties of ZnO thin films prepared by thermal evaporation method. *J. Electron Devices*, 10: 448-455.
- Gao, N., Y.Y. Yan, X.Y. Chen and D.J. Mee, 2011. Superhydrophobic surfaces with hierarchical structure. *Mater. Lett.*, 65: 2902-2905.
- Gao, Y., I. Gereige, A. El Labban, D. Cha and T.T. Isimjan *et al.*, 2014. Highly transparent and UV-resistant superhydrophobic SiO<sub>2</sub>-coated ZnO nanorod arrays. *ACS. Appl. Mater. Interfaces*, 6: 2219-2223.
- Guo, Z., W. Liu and B.L. Su, 2011. Superhydrophobic surfaces: From natural to biomimetic to functional. *J. Colloid Interface Sci.*, 353: 335-355.
- Hiralal, P., C. Chien, N.N. Lal, W. Abeygunasekara and A. Kumar *et al.*, 2014. Nanowire-based multifunctional antireflection coatings for solar cells. *Nanoscale*, 6: 14555-14562.
- Hussain, B., A. Ebong and I. Ferguson, 2015. Zinc oxide as an active n-layer and antireflection coating for silicon based heterojunction solar cell. *Solar Energy Mater. Cells*, 139: 95-100.

- Klochko, N.P., G.S. Khrypunov, V.R. Kopach, I.I. Tyukhov and K.S. Klepikova *et al.*, 2013. Ultrasound assisted nickel plating and silicide contact formation for vertical multi-junction solar cells. *Solar Energy*, 98: 384-391.
- Lam, C.N.C., R. Wu, D. Li, M.L. Hair and A.W. Neumann, 2002. Study of the advancing and receding contact angles: Liquid sorption as a cause of contact angle hysteresis. *Adv. Colloid Interface Sci.*, 96: 169-191.
- Liu, H., L. Feng, J. Zhai, L. Jiang and D. Zhu, 2004. Reversible wettability of a chemical vapor deposition prepared ZnO film between superhydrophobicity and superhydrophilicity. *Langmuir*, 20: 5659-5661.
- Liu, Y., A. Das, S. Xu, Z. Lin and C. Xu *et al.*, 2011. Hybridizing ZnO nanowires with micropylamid silicon wafers as superhydrophobic high-efficiency solar cells. *Adv. Energy Mater.*, 20: 1-5.
- Myint, M.T.Z., G.L. Hornyak and J. Dutta, 2014. One pot synthesis of opposing rose petal and lotus leaf superhydrophobic materials with zinc oxide nanorods. *J. Colloid Interface Sci.*, 415: 32-38.
- Quere, D., 1998. Drops at rest on a tilted plane. *Langmuir*, 14: 2213-2216.
- Shirtcliffe, N.J., G. McHale, S. Atherton and M.I. Newton, 2010. An introduction to superhydrophobicity. *Adv. Colloid Interface Sci.*, 161: 124-138.
- Yan, Y.Y., N. Gao and W. Barthlott, 2011. Mimicking natural superhydrophobic surfaces and grasping the wetting process: A review on recent progress in preparing superhydrophobic surfaces. *Adv. Colloid Interface Sci.*, 169: 80-105.
- Zhang, X.T., O. Sato and A. Fujishima, 2004. Water ultrarepellency induced by nanocolumnar ZnO surface. *Langmuir*, 20: 6065-6067.